

Estimating A Single Molecule's Orientation With Polarized Illumination Microscopy

May 2, 2017

1 Introduction

In this work we evaluate wide-field polarized microscope designs for determining the orientation of single molecules. In section 2 we model the relationship between a molecule's orientation, the microscope geometry, and the measured intensity. In section 3 we present simulation results to show how these microscopes behave, and we compare the ability of several microscope designs to reconstruct the orientation of single dipoles using techniques from estimation theory. Finally, in sections 4 and 5 we summarize our results and present plans for future work.

2 Methods

In this section we model the relationship between a single molecule's orientation, the microscope's geometry, and the measured intensity. We split the model into two parts. First, we develop the illumination model and calculate the excitation efficiency, η_{exc} —the fraction of the maximum power absorbed by the molecule. Next, we develop the detection model and calculate the detection efficiency, η_{det} —the fraction of the power emitted by the molecule that we detect. Finally, we multiply the excitation efficiency and the detection efficiency to find the total efficiency, η_{tot} —a quantity that is proportional to the measured intensity.

2.1 Illumination Model

In this section we model the excitation efficiency of a single molecule with absorption dipole moment $\hat{\mu}_{\text{abs}}$ at the focal point of a condenser. We excite the molecule with Köhler illumination with a linear polarizer in the back focal plane of the condenser. Each point in the back focal plane illuminates the molecule with a polarized plane wave rotated by the condenser, and each polarized plane wave acts on the molecule independently, so we can find the excitation efficiency by integrating over the back focal plane of the condenser. Therefore, the excitation efficiency is

$$\eta_{\text{exc}} = \frac{\int_{\text{bfp}} d\mathbf{r}' |\hat{\mu}_{\text{abs}}^\dagger \hat{\mathbf{A}}_{\text{ffp}}|^2}{\int_{\text{bfp}} d\mathbf{r}'} \quad (1)$$

$$\hat{\mathbf{A}}_{\text{ffp}}(\hat{\mathbf{r}}') = \tilde{\mathbf{R}}(\hat{\mathbf{r}}') \mathbf{A}_{\text{bfp}} \quad (2)$$

where $\hat{\mathbf{A}}_{\text{bfp}}$ is the direction of the polarizer in the back focal plane, $\hat{\mathbf{r}}'$ is the position coordinate in the back focal plane, $\tilde{\mathbf{R}}(\hat{\mathbf{r}}')$ is the position-dependent rotation matrix that rotates the generalized Jones vector (GJV) in the back focal to a GJV in the front focal plane, $\hat{\mathbf{A}}_{\text{ffp}}$ is the GJV in the front focal plane due to the point $\hat{\mathbf{r}}'$ in the back focal plane, $\hat{\mu}_{\text{abs}}$ is the molecule's absorption dipole moment, and † denotes the adjoint operator.

η_{exc} is normalized by the area of the back focal plane so the it can be interpreted as the fraction of the maximum power absorbed by the molecule. If the back focal plane is a pinhole then the molecule is illuminated by a single plane wave. If the plane wave is aligned with the dipole ($\hat{\mathbf{A}}_{\text{bfp}} = \hat{\mu}_{\text{abs}}$) then $\eta_{\text{exc}} = 1$, the most power the dipole can absorb. Opening the aperture or rotating the molecule will decrease the excitation efficiency.

Equation 1 is too computationally expensive to calculate for each illumination and dipole orientation. Instead, we follow [1] and factor the integral so that we can calculate an illumination basis once for each illumination

geometry. The factored form of equation 1 is

$$\eta_{\text{exc}} = \frac{1}{f_{\text{BFP}}} d\mathbf{r}' [\mu_x^2, \mu_y^2, \mu_z^2, \mu_x\mu_y, \mu_x\mu_z, \mu_y\mu_z] \cdot \int_{\text{BFP}} d\mathbf{r}' [|A_x|^2, |A_y|^2, |A_z|^2, 2\text{Re}\{A_x^* A_y\}, 2\text{Re}\{A_x^* A_z\}, 2\text{Re}\{A_y^* A_z\}]^T \quad (3)$$

where

$$\hat{\mathbf{A}}_{\text{ffp}} = A_x \hat{\mathbf{i}} + A_y \hat{\mathbf{j}} + A_z \hat{\mathbf{k}} \quad (4)$$

$$\hat{\boldsymbol{\mu}}_{\text{abs}} = \mu_x \hat{\mathbf{i}} + \mu_y \hat{\mathbf{j}} + \mu_z \hat{\mathbf{k}} \quad (5)$$

We plot the illumination basis elements in figure 1.

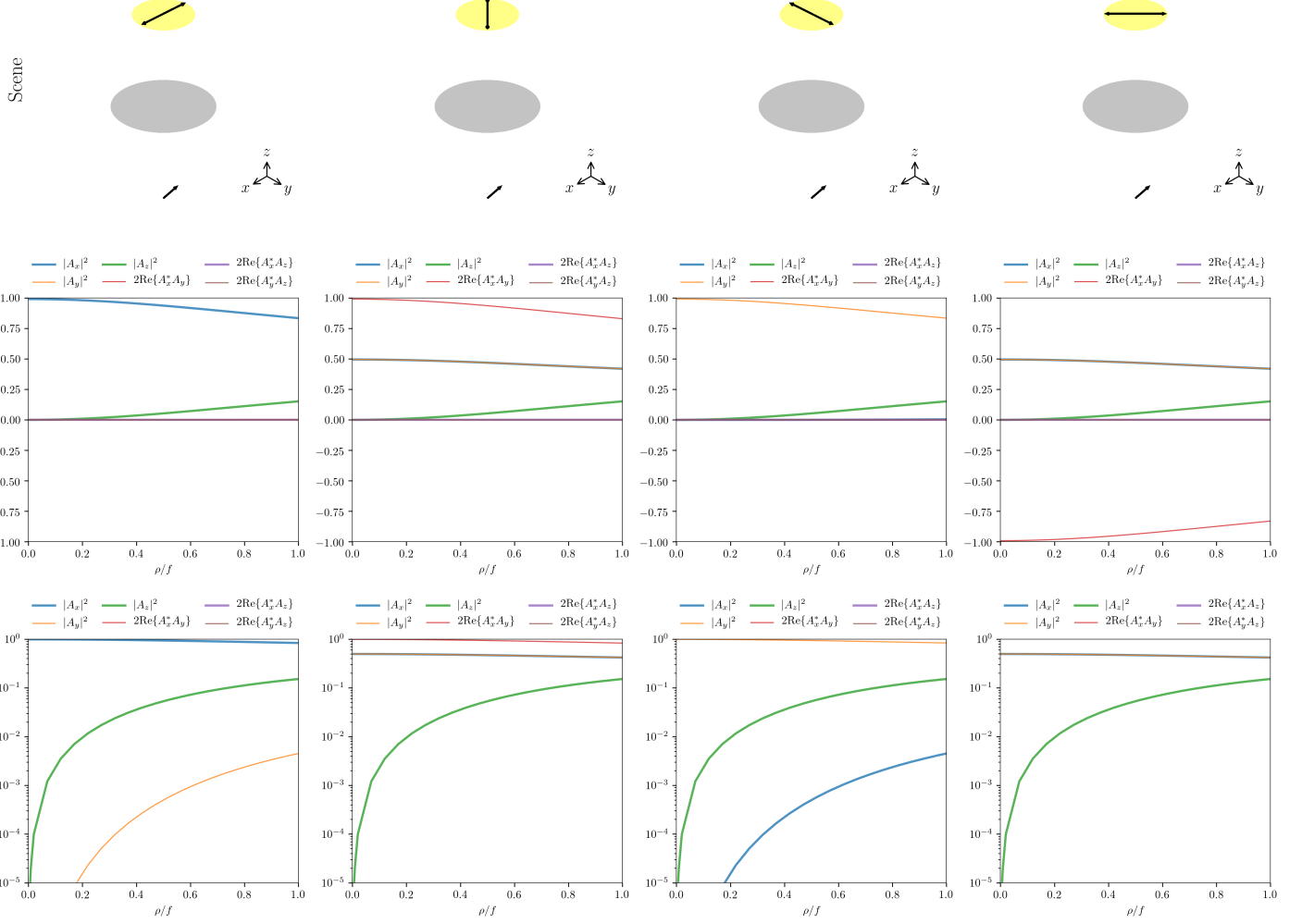


Figure 1: Illumination basis elements as a function of polarization orientation and back focal plane radius. Row 1: schematics of the illumination geometries—a polarizer is placed in the back focal plane of the condenser lens. Row 2 and 3: plots of the illumination basis elements as a function of ρ/f —the ratio of the back focal plane radius to the focal length. The illumination basis elements should be interpreted with equation 3 in view—they do not have a direct physical interpretation. Columns: varying polarization orientations.

2.2 Detection Model

In this section we model the detection efficiency—the fraction of the power emitted by a single molecule that we detect. We follow Fourkas [2] and find that the detection efficiency is

$$\eta_{\text{det}} = 2(A + B \sin^2 \theta) \quad (6)$$

$$A = \frac{1}{4} - \frac{3}{8} \cos \alpha + \frac{1}{8} \cos^3 \alpha \quad (7)$$

$$B = \frac{3}{16} \cos \alpha - \frac{3}{16} \cos^3 \alpha \quad (8)$$

where θ is the angle between the molecule's emission dipole moment $\hat{\mu}_{\text{em}}$ and the detection arm's optical axis, and α is the half angle of the collection cone. See the note set “Inconsistency in rapid determination of the three-dimensional orientation of single molecules” for the derivation of this model. Notice that we're using the corrected versions of Fourkas' variables A and B .

For this work we assume that $\hat{\mu}_{\text{abs}} = \hat{\mu}_{\text{em}}$.

3 Results

3.1 Excitation, Detection, and Total Efficiency

Figure 2 shows representative results of the excitation, detection, and total efficiencies as a function of dipole direction and microscope geometry. Notice that a single frame does not give us enough information to recover a dipole's direction. In the next section we will consider using the information from combinations of single frame microscopes like the ones shown in Figure 2.

3.2 Dipole Orientation Estimates With Multiple Frame Experiments

In this section we combine the results from several single frame microscopes to create multiple frame experiments, and we investigate the possibility of using the information from multiple frames to reconstruct a single molecule's orientation. To assess our ability to reconstruct a molecule's orientation from intensity measurements, we parameterize the molecule's orientation with spherical coordinates ($\hat{\mu}_{\text{em}} = \sin \Theta \cos \Phi \hat{i} + \sin \Theta \sin \Phi \hat{j} + \cos \Theta \hat{k}$), find the minimum variance of an unbiased estimator for these parameters (σ_Θ^2 and σ_Φ^2) using the Cramer Rao lower bound, and calculate a metric we call the solid-angle uncertainty— $\sigma_\Omega = \sin \Theta \sigma_\Theta \sigma_\Phi$. We use σ_Ω as our figure of merit because it is easy to interpret—given a single molecule's orientation and a set of measurements, σ_Ω is the solid angle of the cone of uncertainty about the molecule's reconstructed orientation.

3.3 Single-View Microscope Results

Figure 3 shows the solid-angle uncertainty for multiple-frame, single-view experiments. Each experiment consists of four frames with different polarization orientations and fixed illumination and detection geometry. We used a Poisson noise model with 1000 illuminating photons per frame, a back focal plane radius of $3/10$ the focal length of the condenser, and a detection NA of 1.3.

3.4 Dual-View Microscope Results

Figure 4 shows the solid-angle uncertainty for multiple-frame, dual-view experiments. We've repeated the experiments in the previous section, but now we collect four polarization frames with one view, swap the illumination and detection arms, then collect another four polarization frames. We halved the number of illuminating photons to 500 per frame to allow for a fair comparison between the single arm and dual arm results.

4 Discussion

An ideal microscope geometry would allow us to reconstruct the orientation of a single molecule with a constant solid-angle uncertainty for every orientation of the molecule. We can't accomplish this goal without a large number of detectors at all positions around the dipole, so instead we choose microscope geometries that are experimentally feasible and give us the most uniform solid-angle uncertainty.

Figure 3 shows that single-view microscopes cannot be used to reconstruct single molecules with uniform solid-angle uncertainty. All single-view geometries are degenerate near a plane of molecule orientations. In the epi-detection case the degeneracy occurs near the plane orthogonal to the optical axis. A molecule lying near this plane will give rise to data that cannot be used to determine whether the molecule lies above or below the plane. Lu discussed this degeneracy in detail and developed techniques to avoid reconstruction issues [3]. When the detector is rotated the plane of degeneracy moves but does not disappear. Notice that moving the detector away from epi-detection always decreases the detection efficiency, so there is no advantage to using oblique or orthogonal detection geometries with only one view.

Figure 4 shows that oblique and orthogonal geometries can be advantageous for dual-view microscopes. The first column of Figure 4 shows the epi-detection case with the plane of degeneracy orthogonal to the detection axis. The second and third columns show that rotating the second arm away from the first arm creates a dramatically more uniform solid-angle uncertainty. Between the epi-, 45°-, and ortho-detection geometries, we can see that the 45° detection geometry creates the most uniform solid-angle uncertainty. We note that the results extend symmetrically past angles larger than 90°. For example, 135° detection gives equivalent results to 45° detection, and 135° detection may be more experimentally feasible.

5 Next Steps

Limitations and/or next steps:

1. Both the illumination and detection models use the paraxial approximation. I know how to extend to the high-NA case, but the conclusions in this work do not depend on high-NA lenses. Do you think I should extend now or later?
2. I'm currently only using a Poisson noise model, but I've implemented a Poisson + Gaussian model as well if we'd like results with read-out noise. Read-out noise won't cause any major difference—it will just raise the solid-angle uncertainty baseline.
3. Currently I'm calculating Equation 3 numerically, and I'm getting reasonable results (see Figure 1 and Figure 2). I can write 3 in terms of six integrals, and I think that those integrals will simplify under the paraxial assumption. This may allow us to consider the effect of illumination in closed form. Still investigating.
4. The 45° and 135° cases are identical if the molecule is in a homogeneous environment. I have the tools to consider the case where the molecule is near an interface [1], but I haven't implemented this yet.

Questions:

1. I've parameterized the radius of the back focal plane with ρ/f , the ratio the back focal plane radius to the focal length. Would NA_{illum} be more appropriate?
2. Is 500/1000 illuminating photons per frame appropriate? What are typical read out noise levels?

References

- [1] Adam S. Backer and W. E. Moerner. Extending single-molecule microscopy using optical fourier processing. *The Journal of Physical Chemistry B*, 118(28):8313–8329, 2014. PMID: 24745862.
- [2] John T. Fourkas. Rapid determination of the three-dimensional orientation of single molecules. *Opt. Lett.*, 26(4):211–213, Feb 2001.
- [3] Chun-Yaung Lu and David A. Vanden Bout. Analysis of orientational dynamics of single fluorophore trajectories from three-angle polarization experiments. *The Journal of Chemical Physics*, 128(24):244501, 2008.

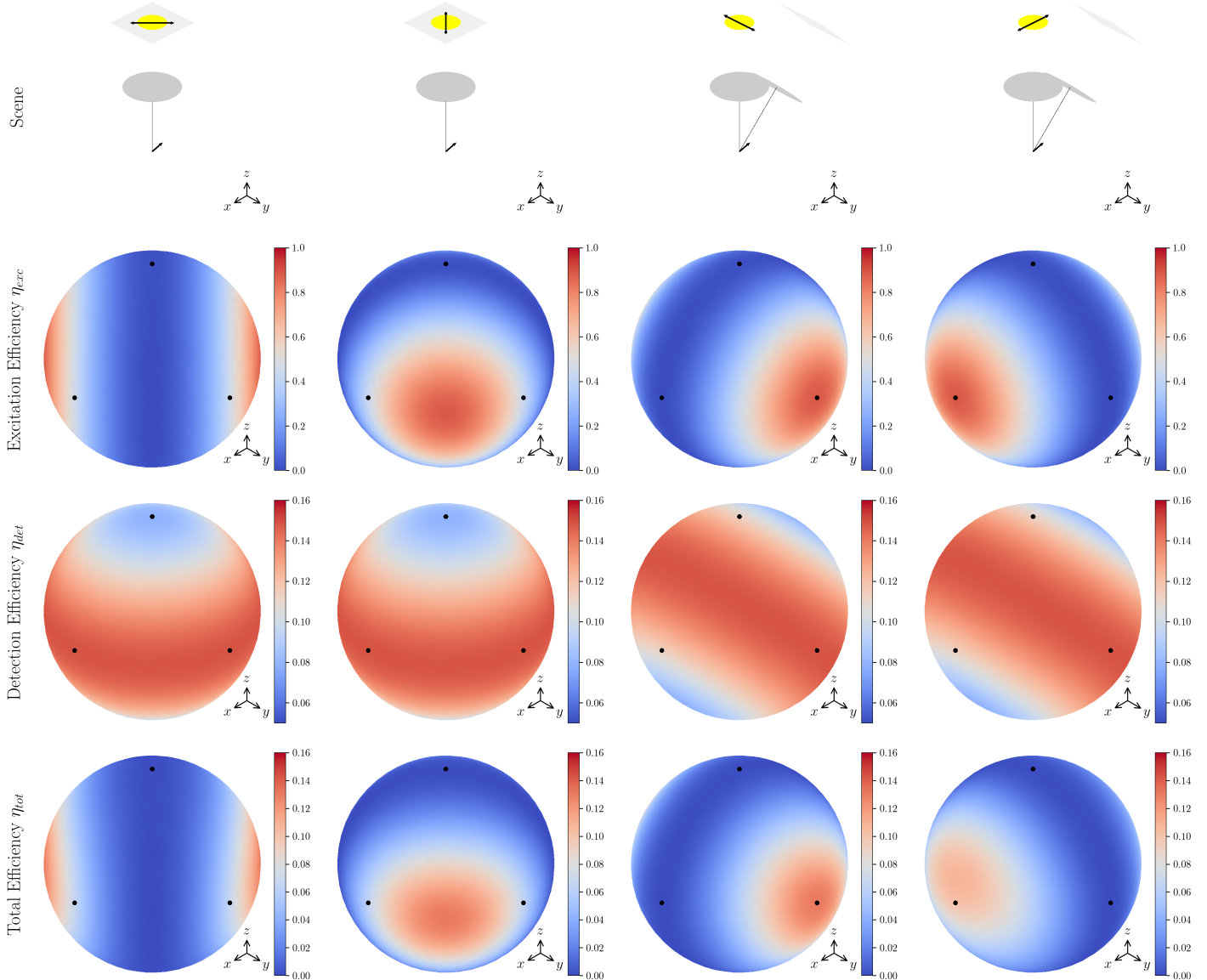


Figure 2: Representative examples of single frame microscopes. Row 1: schematics of the illumination and detection geometries. Rows 2-4: excitation, detection, and total efficiency as a function of dipole direction. The total efficiency is the product of the excitation efficiency and the detection efficiency.

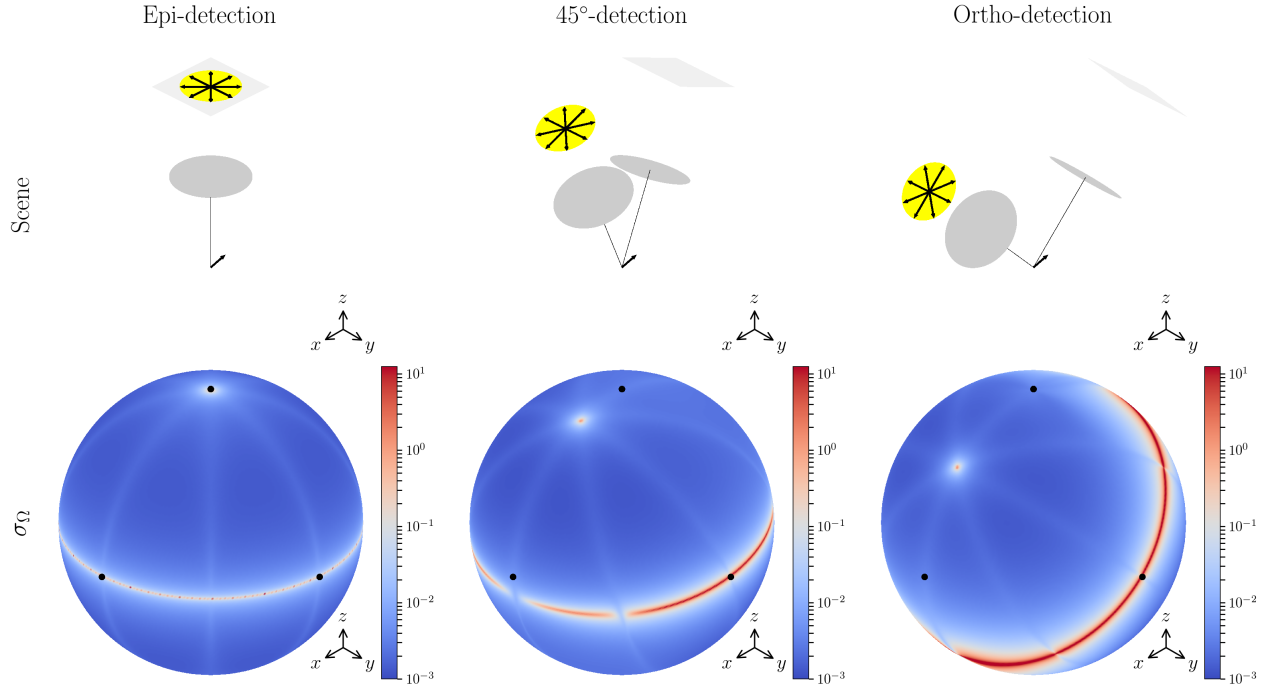


Figure 3: Solid-angle uncertainty for single view multiple frame microscopes. Row 1: schematics of the microscope geometries—we detect four frames with different illumination polarizations. Row 2: solid-angle uncertainty as a function of dipole orientation. A small σ_Ω indicates that the orientation of a dipole oriented along this direction can be precisely recovered from the data collected with this microscope geometry. Columns: varying angles between the illumination and detection arms.

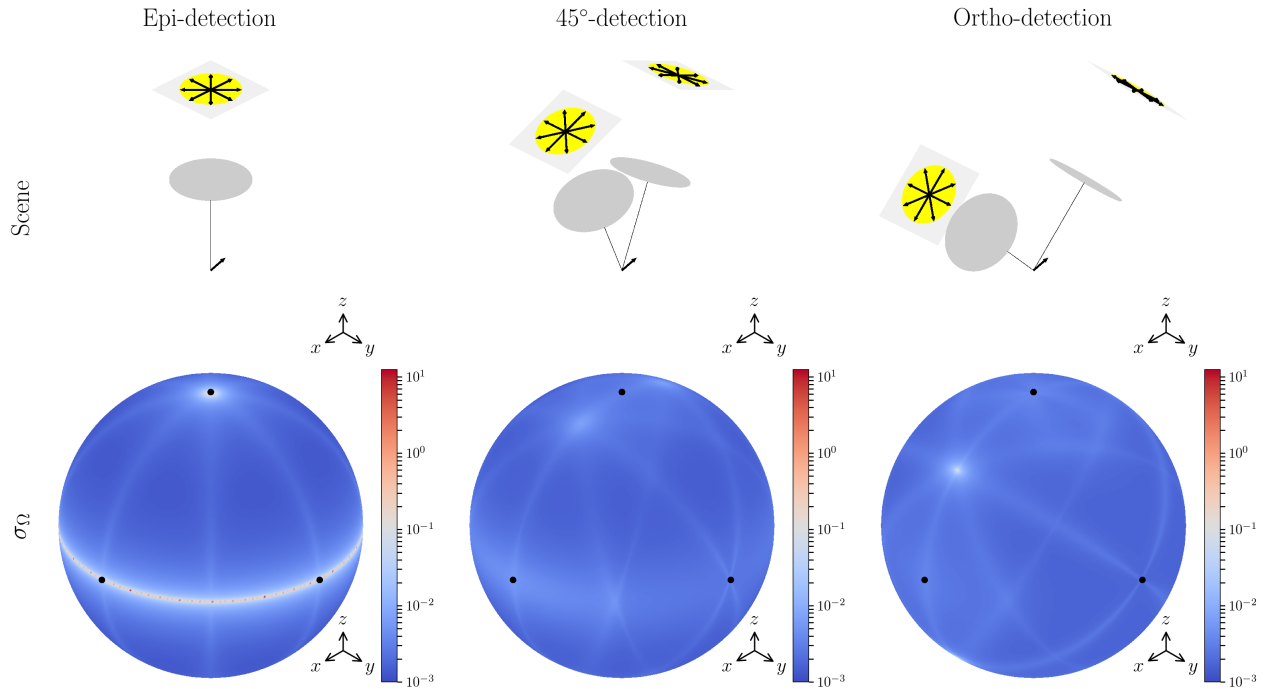


Figure 4: Solid-angle uncertainty for dual view multiple frame microscopes. Same caption as Figure 3 except here we illuminate and detect along both arms. Notice that the 45° detection scheme provides the most uniform solid-angle uncertainty of the designs considered here.